Dielectric Measurement of Liquids Based on the Open-Ended Coaxial Line Reflection Method

Kouji SHIBATA†

ABSTRACT

Various studies of specific absorption rates (SARs) have been carried out with liquid phantoms representing human body tissue to comply with safety standards. As a faithful representation of human body tissue is needed to establish an accurate SAR for measurement, knowledge regarding the precise measurement of sample materials with high permittivity and high loss is very important. In this study, the complex permittivity of a liquid phantom material was measured using the open-ended coaxial line reflection method. The effectiveness of the proposed approach for measuring a liquid phantom with high permittivity and high loss was also confirmed by comparing the measurement results with those obtained using the TMB_{010} circular cavity resonator method and the open-ended cut-off circular waveguide reflection method. As a result, for example, measurement values obtained using each of the three different methods varied within 1.0 for the real part and within 1.5 for the imaginary part when tap water was inserted in the 2.5 GHz frequency band. Meanwhile, it was also confirmed that the variation in complex permittivity values exceeded 2.0 for the real part with a center conductor length of L = 0 mm at a low frequency of around 100 MHz when tap water was inserted. However, the variation in measurement values was reduced to within 1.0 by, for example, extending the length of the center conductor.

Key Words: *Dielectric measurement, liquid, coaxial line, cut-off waveguide, cylindrical cavity resonator, mode-matching technique, mode-matching method, modal analysis, eigenmode expansion, electromagnetic analysis, measurement standards*

1. Introduction

In order to comply with safety standards prescribing limits on exposure to electromagnetic waves, evaluation for the specific absorption rates (SARs) of various radio systems is needed. Meanwhile, methods have been studied for measuring complex permittivity in relation to liquids used as humanoid phantoms [1, 2]. Moreover, the development of techniques for creating new chemical materials based on exposure to electromagnetic waves has accelerated [3]. In research on such microwave chemistry applications, liquids are generally used as solvents for the synthesis of new chemical materials. Accordingly, knowledge of exact material constants for objects to be heated in the frequency band of electromagnetic wave exposure is very important [4].

A reflection constant measuring method involving the use of a coaxial probe is commonly adopted to estimate the complex permittivity of liquids in the MHz and GHz frequency bands [5, 6]. Although this method readily supports broadband estimation of material constants for liquids, a large amount of water is needed to avoid the influence of reflective waves from the vessel bottom. The cavity resonator method can also be used for high-precision measurement [7, 8]. However, as this approach involves the determination of material constants at discrete frequencies in response to the resonant frequency of a cavity resonator, it does not support broadband measurement with a continuous frequency. A transmission constant measuring technique involving the insertion of a liquid sample into a Teflon tube with a waveguide can be used for measurement at a continuous frequency [9], but this method requires consideration for the influence of the

† 工学部工学科電気電子通信工学コース 教授

medium into which the sample is placed. A transmission constant measuring method involving the insertion of sample materials into a coaxial line [10] and a reflection constant measuring method involving the insertion of sample materials into a cylindrical cavity [11] can be adopted for broadband measurement, but these approaches require consideration for the influence of liquid spillage. A cross-shaped coaxial probe can be used for simple measurement of complex permittivity, but material constant data on a known material is required as standard with this approach [12].

The author previously proposed broadband measurement of complex permittivity for liquids based on the reflection coefficient using a coaxial feed-type open-ended cut-off circular waveguide with an SMA connector [13]-[15]. The validity of the proposed method was confirmed in the microwave band by comparing its measurement results with those of the circular cavity method in the 2.5GHz band [8]. Based on the outcomes of these fundamental studies, frequency characteristics associated with the complex permittivity of certain types of high-loss liquids at frequencies ranging from 50 MHz to 3.0 GHz were measured over a broad frequency range. As a result, the effectiveness of the proposed approach for measuring liquids was confirmed [16].

However, measurement with this approach was performed with the tip of the coaxial line open, and it can be assumed that measurement precision will deteriorate significantly due to large variations in the results of complex permittivity estimation in the ultra-low frequency band [16]. Moreover, measurement results previously obtained by the author's research group using the proposed approach (cut-off circular waveguide reflection method) need to be verified based on comparison with those of another measurement method or another approach at very low frequency.

Accordingly, the complex permittivity of certain types of high-loss liquids were measured in this study to validate past measurement results and achieve progress in measurement precision using an open-ended circular waveguide loaded coaxial line [17, 18]. The repeatability, validity and precision of measurement results obtained using the method presented here were therefore considered by comparing them with those of other methods. Measurement results and outcomes obtained using another measurement method were also compared to support evaluation of the proposed technique's effectiveness. Finally, the frequency characteristics of the complex permittivity of liquids were confirmed based on measurement over a broad frequency range.

As a result, variations in measured complex permittivity values obtained with the proposed method decreased with the length of the center conductor in the cylindrical cavity of the material insertion space in the low-frequency band because the matching condition was improved by a reduction in reflection waves. It can be concluded that measurement precision was therefore also improved in the low-frequency band with the proposed structure.

2. Measurement procedure

This section describes complex permittivity measurement using the proposed method. The method adopted was that of Reference [17], which enables high-precision measurement of material constants based on the application of electromagnetic analysis for calculation of S_{11} as proposed by an NIST research group. The validity and accuracy of complex permittivity measurement mostly at low frequencies using this method were verified by comparing the results with those obtained using the author's previously proposed approach. The measurement jig for liquid insertion is made from a cut piece of worked brass and an SMA connector. S_{11} calibration must be performed before the measurement jig is mounted when input impedance is measured using a vector network analyzer (VNA). The jig, shown in Figure 1, was expected to have input impedance approaching 50Ω, as the electromagnetic wave is absorbed by the liquid when the center conductor is dipped in liquid because it projects out into the cylindrical cavity. A cross-section of the jig is also shown in Fig. 2. The sample insertion slot has a patulous form. The jig is filled with liquid at the coaxial line part because the center conductor of the SMA connector projects into the cylindrical cavity space (in contrast to the situation with the open-ended cut-off circular waveguide method).

In this measurement condition, input impedance was measured when liquid was inserted into the measurement jig with the tip of the cylindrical cavity open, as shown in Figure 2. The top face of the jig was left open to facilitate sample insertion. Input impedance is then measured at the front of the sample material

upon its insertion into the measurement jig using a vector network analyzer after the jig is attached to a measurement cable connected to the network analyzer (see Figs. 1 to 3). The reference plane is then moved using a VNA electrical delay function so that the input impedance is ∞ Ω on the Smith chart when the measurement jig is attached. When actual measurement is made, a coaxial line attenuator (6 dB) is connected to the front of the measurement jig to reduce the influence of reflection waves on the measurement results with this setup (see Figs. 1 to 3). Finally, the complex permittivity of the sample material is estimated based on an inverse problem to coincide with the calculated input impedance and the results of input impedance measurement. The coaxial cable is shown connected to port 2 in Fig. 3 only because this measurement setup is often used to measure S_{21} for microwave components such as filters; this port in fact plays no part in the proposed method. In addition, the complex permittivity of the inserted sample material must be estimated from the measured input impedance as an inverse problem. This work is performed using the 2D Newton-Raphson method.

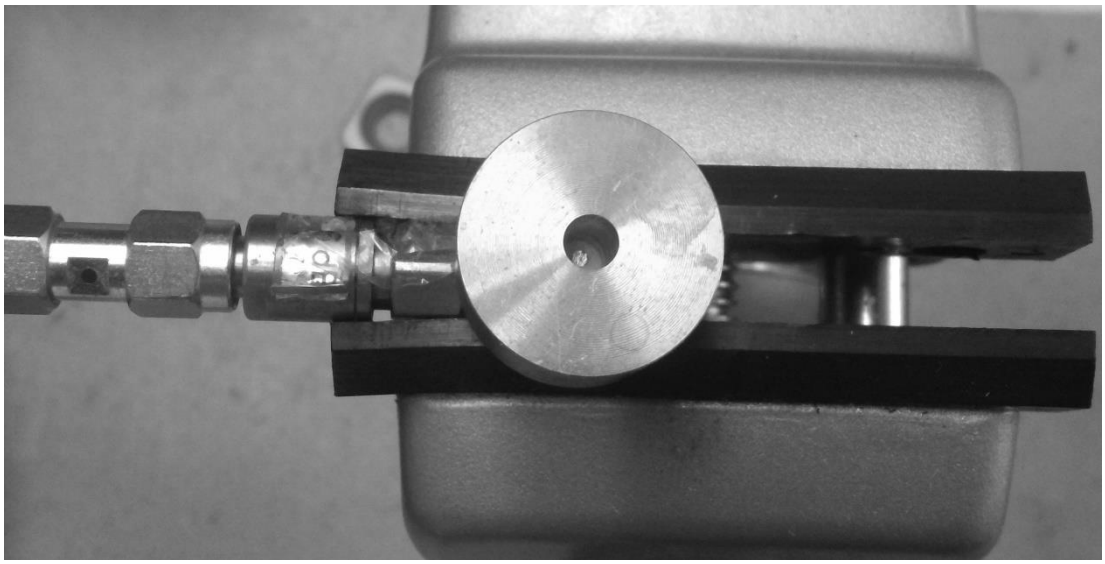

Figure 1. Measurement jig

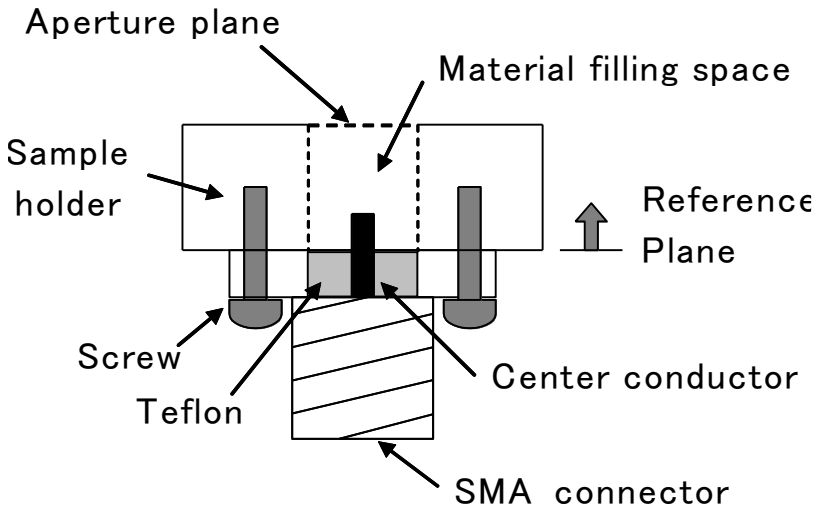

Figure 2. Measurement jig cross section

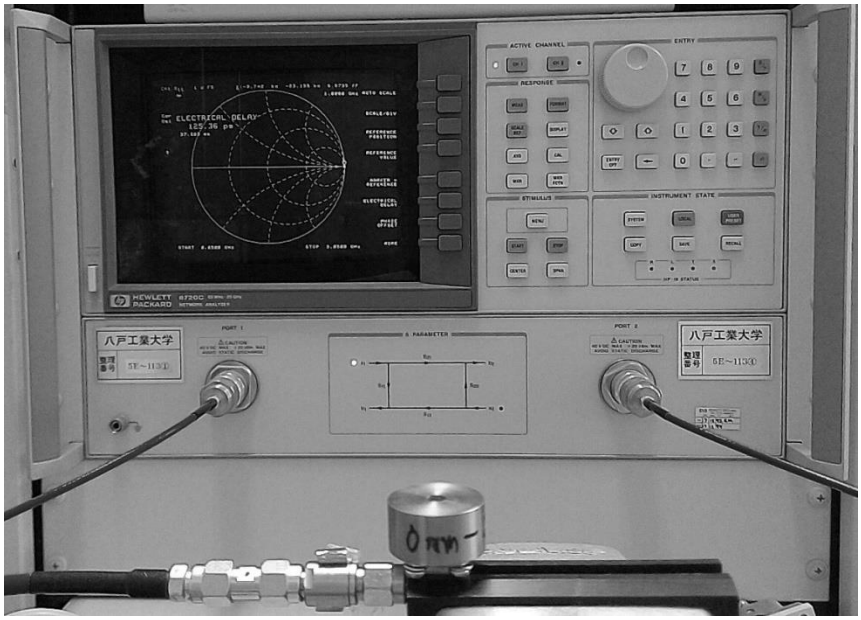

Figure 3. Measurement setup

3. Calculation of input impedance

In the proposed method, complex permittivity must be estimated by comparing measured and calculated S-parameter values. Accordingly, S-parameters of the structure with a liquid-filled jig need to be computed under conditions identical to those of the structure used to measure these values. The analytical model used for S-parameter calculation in the study is described below.

Region 1 (the front of z = L), Region 2 (z = 0 to L) and Region 3 (z = L to L_1) in Fig. 4 correspond to Fig. 2 as follows: Region 1: filling of the coaxial line of the SMA connector with Teflon (the front of the reference plane); Region 2: filling of the coaxial line with liquid due to the center conductor's projection into the sample insertion space; and Region 3: filling of only the cylindrical cavity part with liquid. The z= L_1 plane in Fig. 4 also corresponds to the aperture plane in Fig. 2. First, it was assumed that regions 1 and 2 were filled with Teflon and liquid, respectively, in an analytical model of a coaxial line with an open-ended termination as shown in Fig. 4. Region 3 (a circular waveguide section) was also assumed to be filled with liquid based on the insertion of a sample material. However, electromagnetic waves propagated in the cut-off mode in region 3 because this section was a cut-off region when the bore diameter of the cylinder was small enough in relation to the wavelength. Next, the electromagnetic waves of each of regions 1, 2 and 3 in the analytical model were expressed using an equation containing Bessel functions of the cylindrical coordinate system [17, 18]. Then, formulation was performed using the Galerkin method based on the orthogonality of the Bessel function to simultaneous equations. These equations were obtained by applying the continuity condition to the tangential components of the electromagnetics for each region. Thus, the reflection constant at the reference plane (z = 0) as seen from the right-hand side in Fig. 4 can be calculated using Equation 1 [17, 18].

$$\boldsymbol{\Gamma} = \boldsymbol{P}^{-1} \cdot \boldsymbol{T} \quad \text{... (1)}$$

$\boldsymbol{P}$ and $\boldsymbol{T}$ here are matrices, and become

$$\boldsymbol{P} = \boldsymbol{M8} \cdot \boldsymbol{M6} + \boldsymbol{M9} \cdot \boldsymbol{M7} \quad \text{... (2)}$$

$$\boldsymbol{T} = -\boldsymbol{M8} \cdot \boldsymbol{C} - \boldsymbol{M9} \cdot \boldsymbol{D} \quad \text{... (3)}$$

These matrix element become

$$\boldsymbol{M6} = \boldsymbol{M6}_{\boldsymbol{mn}} = \frac{1}{2}\left(1 - \frac{\varepsilon_{r1} \cdot \gamma_{2n}}{\varepsilon_{r2} \cdot \gamma_{1n}}\right) \cdot \delta_{mn} \quad \text{... (4)}$$

$$\boldsymbol{M7} = \boldsymbol{M7}_{\boldsymbol{mn}} = \frac{1}{2}\left(1 + \frac{\varepsilon_{r1} \cdot \gamma_{2n}}{\varepsilon_{r2} \cdot \gamma_{1n}}\right) \cdot \delta_{mn} \quad \text{... (5)}$$

$$\boldsymbol{M8} = \boldsymbol{M3} \cdot \boldsymbol{M1} - \boldsymbol{M4} \quad \text{... (6)}$$

$$\boldsymbol{M9} = \boldsymbol{M3} \cdot \boldsymbol{M2} + \boldsymbol{M5} \quad \text{... (7)} \quad (m, n = 0, 1, 2, \ldots M, N)$$

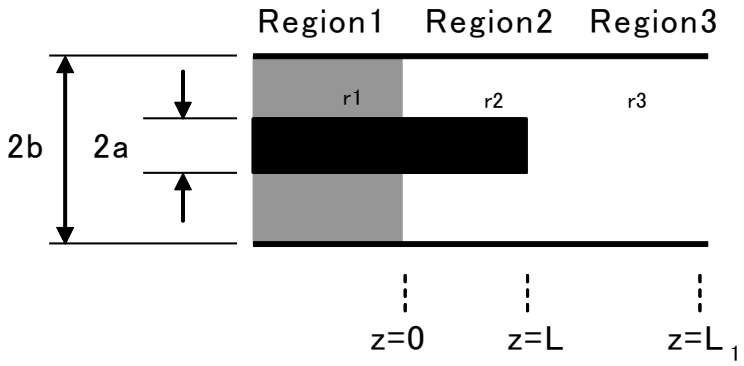

Figure 4. Analytical model

where ε_{r1} and ε_{r2} are the complex relative permittivity values for regions 1 and 2, respectively, δ_{mn} is the Kronecker delta function, and γ_{1n} and γ_{2n} are the propagation constants for each region. These values are used to create the equation shown below for the TEM mode with n = 0 in the region of i = 1, 2.

$$\gamma_{i0} = j\frac{\omega\sqrt{\varepsilon_{ri}}}{c_{vac}} \quad \text{... (8)}$$

In addition, C_{vac} is the speed of light, and ε_{ri} is the relative permittivity of each region. Meanwhile, the propagation constant is as shown below in the region of i = 1, 2 for n > 0. Meanwhile, the propagation constant is as shown below in the region of i = 1, 2 for n > 0.

$$\gamma_{in} = j\sqrt{\varepsilon_{ri} \cdot \mu_{ri} \cdot \frac{\omega^2}{c_{vac}^{\ 2}} - k_{in}^{\ 2}} \quad \text{... (9)}$$

where ε_{ri} and μ_{ri} are the relative permittivity and permeability, respectively, in each region. γ_{3m} is also as shown below when the inside of the root is negative in the region of i = 1, 2 and the electromagnetic wave of region 3 is in the cut-off mode for all n values.

$$\gamma_{in} = \sqrt{k_{in}^{\ 2} - \varepsilon_{ri} \cdot \mu_{ri} \cdot \frac{\omega^2}{c_{vac}^{\ 2}}} \quad \text{... (10)}$$

Additionally, k_{in} is determined as the n-th root of the following equation:

$$J_0\left(k_{in} \cdot b\right)Y_0\left(k_{in} \cdot a\right) - Y_0\left(k_{in} \cdot b\right)J_0\left(k_{in} \cdot a\right) = 0 \quad \text{... (11)}$$

where J_0 and Y_0 are Bessel functions of the first and second kind. Moreover, ***C*** and ***D*** are

$$\boldsymbol{C} = \boldsymbol{C_n} = \frac{1}{2}\left[\delta_{n0} \cdot \left(1 + \frac{\varepsilon_{r1} \cdot \gamma_{2n}}{\varepsilon_{r2} \cdot \gamma_{1n}}\right)\right] \text{... (12)}$$

$$\boldsymbol{D} = \boldsymbol{D_n} = \frac{1}{2}\left[\delta_{n0} \cdot \left(1 - \frac{\varepsilon_{r1} \cdot \gamma_{2n}}{\varepsilon_{r2} \cdot \gamma_{1n}}\right)\right] \quad (n = 0, 1, 2,\ldots) \text{ ... (13)}$$

Next, ***M1*** to ***M3*** are calculated using the following equations:

$$\boldsymbol{M1} = \boldsymbol{M1_{mn}} = e^{+\gamma_{3m}L} \cdot e^{-\gamma_{2n}L} \cdot \left\langle G_m R_n \right\rangle \text{ ... (14)}$$

$$\boldsymbol{M2} = \boldsymbol{M2_{mn}} = e^{+\gamma_{3m}L} \cdot e^{+\gamma_{2n}L} \cdot \left\langle G_m R_n \right\rangle \text{ ... (15)}$$

$$\boldsymbol{M3} = \boldsymbol{M3_{nm}} = e^{-\gamma_{3m}L} \cdot \left\langle G_m R_n \right\rangle \cdot \frac{\gamma_{2n} \cdot \varepsilon_{r3}}{\gamma_{3m} \cdot \varepsilon_{r2}} \text{ ... (16)} \quad (m = 1, 2, 3\ldots, n = 0, 1, 2\ldots, MI_{00} - MI_{0n} = 0)$$

M4 and ***M5*** can also be calculated as

$$\boldsymbol{M4} = \boldsymbol{M4_{mn}} = e^{-\gamma_{2n}L} \cdot \delta_{mn} \text{ ... (17)}$$

$$\boldsymbol{M5} = \boldsymbol{M5_{mn}} = e^{+\gamma_{2n}L} \cdot \delta_{mn} \quad (m, n = 0, 1, 2,\ldots M, N) \text{ ... (18)}$$

where ε_{r3} is the complex permittivity of Region 3.

$\left\langle G_m R_n \right\rangle$ is expressed as a product of the normalization constant and the coupling integral as

$$\left\langle G_m R_n \right\rangle = S3_m \cdot D3_{mn} \text{ ... (19)}$$

$S3_m$ in these formulation elements is calculated as

$$S3_m = \frac{\sqrt{2}}{b \cdot J_1\left(k_{3m} \cdot b\right)} \quad (m = 1, 2, 3, \ldots M) \text{ ... (20)}$$

where $\boldsymbol{k_{3m}}$ is determined as the root of $J_1\left(k_{3m} \cdot b\right) = 0$. where J_1 is a Bessel function of the first kind.

$\boldsymbol{D3_{mn}}$ can also be calculated with n = 0 as

$$D3_{m0} = C_0 \cdot J_0\left(k_{3m} \cdot a\right) \cdot \frac{1}{k_{3m}} \quad \text{... (21)}$$

where C_0 can be defined using

$$C_0 = \frac{1}{\sqrt{ln\left(b / a\right)}} \quad (m = 1, 2, 3, \ldots M) \text{ ... (22)}$$

$\boldsymbol{D3_{mn}}$ can also be calculated with n≠0 as

$$D3_{mn} = \frac{2}{\pi} \cdot \frac{C_n}{k_{2n}} \cdot \frac{k_{3m}}{{k_{2n}}^2 - {k_{3m}}^2} \cdot \frac{1}{J_0\left(k_{2n} \cdot b\right)} \cdot \left[J_0\left(k_{3m} \cdot b\right) J_0\left(k_{2n} \cdot a\right) - J_0\left(k_{3m} \cdot a\right) J_0\left(k_{2n} \cdot b\right)\right] \text{ ... (23)}$$

(under the condition that $n = 1, 2, \ldots N$, $m = 1, 2, \ldots M$)

where C_n can be defined using

$$C_n = \frac{\pi \cdot k_{1n}}{\sqrt{2}} \frac{1}{\sqrt{\frac{{J_0}^2\left(k_{1n} \cdot a\right)}{{J_0}^2\left(k_{1n} \cdot b\right)} - 1}} \quad (n = 1, 2, 3, \ldots N) \text{ ... (24)}$$

k_{1n} and k_{2n} are the eigenvalues of the coaxial structure shown in Fig. 4. Accordingly, the input impedance on the z = 0 plane as seen from the right-hand side of Fig. 3 can also be calculated easily with the reflection constant using Eq. (1). In addition, Eq. (1) – (24) are based on refinement of the formulation presented in Reference [17]. These procedures for S-parameter formulation and calculation are generally called the Mode Matching Method (or the Mode Matching Technique).

When Eq. (1) is iterated, the electro-magnetic fields for each region are expressed as the sum of a finite series to satisfy the continuity condition of the analytical model. Accordingly, the choice of sufficiently large values for the M-by-N matrix of M6 in Equation (4) is needed for convergence toward the S_{11} value by satisfying the simultaneous equation with regard to numerous other higher modes in actual numerical calculation. In this study, the convergence of S_{11} was pre-checked under the condition of N = N = 100. Accordingly, the subsequent calculation of S_{11} was made under the condition that M = N = 100 for each of Equations (1) – (24).

4. Inverse problem

In this approach, complex permittivity is estimated as an inverse problem by comparing the measured input impedance with the calculated result. Accordingly, the inverse problem must be solved as the function of two variables to the assigned equation. In this case, the Newton-Raphson method [19, 20] is applied to the above operation. Complex permittivity is thus determined to minimize residual error using default values for implementation of the following equation as iterative calculation:

$$\begin{bmatrix} \Delta\varepsilon_1 \\ \Delta\varepsilon_2 \end{bmatrix} = \begin{bmatrix} \frac{\partial f_1}{\partial \varepsilon_1} & \frac{\partial f_1}{\partial \varepsilon_2} \\ \frac{\partial f_2}{\partial \varepsilon_1} & \frac{\partial f_2}{\partial \varepsilon_2} \end{bmatrix}^{-1} \cdot \begin{bmatrix} -f_1\left(\varepsilon_1', \varepsilon_2'\right) \\ -f_2\left(\varepsilon_1', \varepsilon_2'\right) \end{bmatrix} \text{ ... (25)}$$

where $\partial f_1/\partial \varepsilon_1$ is the ratio of the minor changed real value ε_1 of complex permittivity to the minor changed value of the input admittance as calculated using Eq. (1). $f_1(\varepsilon_1', \varepsilon_2')$ and $f_2(\varepsilon_1', \varepsilon_2')$ are the real and imaginary parts of the input impedance calculated using Eq. (1) when the default value of complex permittivity is input. Accordingly, $\Delta\varepsilon_1$ and $\Delta\varepsilon_2$ (correction values for the real and imaginary parts of complex permittivity) are determined via the above calculation process. The complex permittivity of the sample material is therefore converged to reach the solution by correcting the complex permittivity using $\Delta\varepsilon_1$ and $\Delta\varepsilon_2$, and Eq. (1) is then iterated repeatedly. For real estimate work, complex permittivity can be estimated at a given specific frequency using results obtained from the cavity resonator method or other approaches. Iterative calculation is expected to result in rapid convergence with this used as the default.
In addition, the default value of complex permittivity for the inverse problem is used for rapid convergence when estimation is performed with the previous frequency.

5. Fundamental study

There are two differences regarding the analytical structure conditions between the two methods of complex permittivity measurement for liquids, the method newly evaluated in this study (the open-ended coaxial line reflection approach [17]) and the method used in reference research (the open-ended cut-off circular waveguide reflection approach [14] – [16]):

1. Both the open-ended cylindrical cavity part and the coaxial part inside the measurement jig are filled with liquid when Eq. (1) above is used. Meanwhile, the structure of the reference formulation [15] is not filled with liquid at the coaxial line part.

2. In formulation for the mode-matching method, the open-ended cylindrical waveguide part on the tip of the coaxial line is described using only the evanescent mode when Eq. (1) above is used. Meanwhile, this part is described using the PMC (perfect magnetic condition) via the cut-off circular waveguide with the reference formulation [15].

Accordingly, the inner structure and the method used to compute S_{11} with the open-ended coaxial line reflection method correspond to those outlined in Reference [17].
The measurement jig was first filled with tap water with the length of the coaxial line's center conductor at L = 0.00 mm. Although Eq. (1) is used for this measurement and calculation, the structure is not filled with liquid at the coaxial line part. Next, complex permittivity was estimated as an inverse problem using the newly evaluated method and the reference method [14] – [16] by performing multiple measurements of input impedance with tap water at a frequency of 2.49806 GHz with values of 2b = 4.10 mm, 2a = 1.30 mm, d = 5.00 mm and ε_{rl} = 2.05. Table 1 summarizes the means of the measurement results obtained using the newly evaluated open-ended coaxial line reflection method along with those obtained using the open-ended cut-off circular waveguide reflection method [14] – [16] and the TM_{010} cylindrical cavity resonator method [8, 14, 15] also at a resonant frequency of 2.49806 GHz for the cavity resonator. The measurement jig was filled with liquid again, and the dielectric constant was measured five times using the cut-off circular waveguide reflection method and five times using the cylindrical cavity resonator method. The ambient temperature was 22.4°C for input impedance measurement with the cut-off circular waveguide reflection method and the reference method [14, 15] and 20.2°C for measurement with the cavity resonator method. The mean value obtained with the proposed method was 72.87 ± 1.03 – j6.98 ± 0.39. The value for the real part of the complex permittivity was close to those obtained with the cut-off circular waveguide reflection method [14] – [16] (73.55 ± 0.93 – j8.49 ± 0.41) and the cavity resonator method (73.20 ± 0.4 – j7.50 ± 0.8) at a frequency of 2.49806 GHz. The difference of around 1.51 observed for the imaginary part with the different methods may be attributable to temperature differences during input impedance measurement. As a result, each estimated value of permittivity for tap water came within 0.4 of the mean (73.2) of the three measurement methods for the real part. Next, methanol, ethanol and isopropanol (IPA)

samples were inserted into the jig, their input impedances were measured three times, and complex permittivity was estimated from each value with the length of the coaxial line's center conductor at L = 0.00 mm. This structure was also not filled with liquid at the coaxial line part, and the measurement frequency for input impedance using the proposed method was the same as that for measurement using the cavity resonator method. Tables 2 to 4 show the estimation results obtained with the newly evaluated method with L = 0.00mm, the measurement results obtained with the open-ended cut-off circular waveguide reflection method and those obtained with the TM_{010} cylindrical cavity resonator method. The outcomes show that the measurement results obtained using the proposed method with L = 0.00mm are relatively close to those of the open-ended cut-off circular waveguide reflection method [14] – [16] and the TM_{010} cylindrical cavity resonator method [8]. In particular, Table 2 indicates that each estimated value for the real part of permittivity for methanol came within 1.0 of the mean (22.2) of the three measurement methods. Moreover, the measurement values obtained with the proposed method corresponded closely to those obtained with the cut-off circular waveguide reflection method (within 0.2 for the imaginary part). However, the estimated value for the imaginary part obtained with the cavity resonator method was about 2.0 lower than those of the other methods. Next, Table 3 indicates that each estimated value for the real part of permittivity for ethanol was within 0.7 of the mean (6.7) obtained with the three measurement methods. Meanwhile, each estimated value was within 0.6 of the mean (7.3) obtained with the three measurement methods for the imaginary part. Finally, Table 4 also indicates that each estimated value for both the real and imaginary parts for isopropanol was close to the mean value obtained with the three measurement methods. In addition, the variation in measurement values for both the real and imaginary parts were relatively small in the 2.5 GHz band. These values for tap water obtained using both the proposed method with the length of the coaxial line's center conductor at L = 0.00 mm and the open-ended cut-off waveguide reflection method as shown in Table 1 decreased to 1.0 for the real part and 0.4 for the imaginary part. Similarly, the variation in all measurement values for methanol as shown in Table 2 decreased to 1.0 for the real part and 0.4 for the imaginary part. Thus, we can also conclude that this value is typically small. Moreover, the variation in measurement values for ethanol and isopropanol obtained using both the newly evaluated method with the length of the coaxial line's center conductor at L = 0.00 mm and the open-ended cut-off waveguide reflection method as shown in Tables 3 and 4 were also small. The reason for this is that the electromagnetic wave propagated to the material boundary despite the fact that the length of the center conductor was L = 0.00 mm because the wavelength decreased at high frequencies. Accordingly, input impedance approached 50Ω when the sample liquid was inserted. The difference between the values obtained with each measurement method may also be attributable to temperature differences during input impedance measurement [21].

Table 1. Complex permittivity of tap water (at 2.49806 GHz)

Newly evaluated coaxial line method [17]	Cut-off circular waveguide reflection method [14] – [16]	TM_{010} cylindrical cavity resonator method [8]
72.87 ± 1.03 – j6.98 ± 0.39	73.55 ± 0.93 – j8.49 ± 0.41	73.2 ± 0.4 – j7.5 ± 0.8

Table 2. Complex permittivity of methanol (at 2.5314 GHz)

Newly evaluated coaxial line method [17]	Cut-off circular waveguide reflection method [14] – [16]	TM_{010} cylindrical cavity resonator method [8]
23.30 ± 0.43 – j13.58± 0.55	21.33 ± 0.50 – j13.77 ± 0.10	22.1 ± 1.3 – j11.4 ± 2.1

Table 3. Complex permittivity of ethanol (at 2.5395 GHz)

Newly evaluated coaxial line method [17]	Cut-off circular waveguide reflection method [14] – [16]	TM_{010} cylindrical cavity resonator method [8]
7.39 ± 0.05 – j7.92 ± 0.14	6.26 ± 0.18 – j7.13 ± 0.18	6.3 ± 0.3 – j6.8 ± 0.3

Table 4. Complex permittivity of isopropanol (IPA) (at 2.5415 GHz)

Newly evaluated coaxial line method [17]	Cut-off circular waveguide reflection method [14] – [16]	TM_{010} cylindrical cavity resonator method [8]
3.06 ± 0.08 – j2.97 ± 0.12	3.24 ± 0.19 – j3.04 ± 0.05	3.5 ± 0.5 – j3.0 ± 0.1

6. Influence of material space depth in the coaxial line part

The complex permittivities of tap water, methanol, ethanol and isopropanol were then also measured numerous times with the measurement jig filled with liquid to the coaxial line section (Fig. 3) with a center conductor length of 0 to 2.00 mm. Here, the inner and outer conductor diameters were 2a = 1.30 mm and 2b = 4.10 mm, respectively, when complex permittivity was measured using the open-ended coaxial line reflection method. Tables 5 to 8 show estimation results obtained with the newly evaluated method, measurement results obtained with the TM_{010} cylindrical cavity resonator method [8], and those obtained with the open-ended circular cut-off waveguide reflection method [14], [15] in the 2.5-GHz band. The measurement results of the newly evaluated method closely match those of the cavity resonator method and those of the open-ended cut-off circular waveguide reflection method despite center conductor length (material insertion part) variations of L = 0 to 2 mm.

A value of L = 0.00 mm for the center conductor of the coaxial line with the proposed method in Tables 5 – 8 indicates that input impedance was calculated using Eq. (1). However, as the center conductor was not projected into the cylindrical cavity space, these conditions were the same as those with the jig for the open-ended cut-off circular waveguide reflection method [14] – [16]. The results confirm the effectiveness of reflection constant calculation for the analytical model using the mode-matching method with liquid inserted to the coaxial line part rather than only to the open-ended cylindrical cavity part. Specifically, first, measurement variation in the real part of permittivity was about 1.1 from the mean (73.1) with varying center conductor lengths (d [mm]) when tap water was inserted, as shown in **Table 5**. Meanwhile, variation in the estimated values of permittivity was 0.27 and 0.08 for each length of the center conductor when input impedance was measured repeatedly under the conditions of L = 1.00 and 2.00 mm, respectively. Accordingly, the results confirmed that the variation in measurement values decreased as the length of the center conductor increased. Moreover, the mean value obtained with the three different measurement methods was 73.3. Accordingly, each measurement value indicates that the difference in permittivity was within 0.3. However, the difference in relative permittivity approached 1.0 under the condition of L = 1.00 mm. Accordingly, there is a clear need for ongoing study in the near future of the factors contributing to differences in each measurement value.

Meanwhile, the variation in measurement values for the imaginary part of permittivity was about 1.1 from the mean (7.9) with varying center conductor lengths (d [mm]). Moreover, the variation in the estimated values of permittivity was 0.47 when input impedance was measured repeatedly under the condition of L = 2.00 mm. It was not confirmed that the improvement in variation was caused by extending the center conductor length at a high frequency of 2.5 GHz with tap water inserted. Meanwhile, the mean value for the imaginary part with the three different measurement methods was 8.0. Accordingly, each measurement value indicates that the difference in permittivity was within 0.5.

Next, measurement variation in the real part of permittivity value was about 0.7 from the mean (22.6) with varying center conductor lengths (d [mm]) with methanol inserted, as shown in **Table 6**. Meanwhile, the values for the real part of permittivity under the condition of L = 1 and 2 mm were closer to each other than for L = 0.00 mm. Moreover, the variation in the estimated values of permittivity was 0.06 when input impedance was measured repeatedly under the condition of L = 2.00 mm. We can assume that this value is typically small. Therefore, it was confirmed that the value when the center conductor length is longer is the more reliable value. Moreover, the mean value of the three different measurement methods was 21.8. Accordingly, each measurement value indicated that the difference in permittivity was within 0.5. Meanwhile, the variation in the measurement values of the imaginary part was about 0.5 from the mean (13.1) with varying center conductor lengths (d [mm]). However, the variation in the estimated values was 0.17 when

input impedance was measured repeatedly under the condition of L = 2.00 mm. Thus, we can also assume that this value is typically small. Moreover, the mean value obtained with the three different measurement methods was 12.8. Thus, the difference was around 1.4 from the value of the imaginary part with each method.

Next, the estimated value for the real part using the coaxial line reflection method with ethanol inserted was approximately 1.0 larger than the value obtained with the other two measurement methods, as shown in **Table 7**. Meanwhile, the difference in each measurement value was within 0.06 of the mean (7.42) regardless of changes in the center conductor length. Moreover, the deviation in the estimated value of permittivity was 0.07 when input impedance was measured repeatedly under the condition of L = 2.00 mm. We can assume that this value is typically small. Therefore, it was concluded that the value obtained using the coaxial line reflection method was more reliable with ethanol inserted in the 2.5 GHz band. Meanwhile, the measurement variation for the imaginary part was about 0.4 from the mean (7.5) with varying center conductor lengths (d [mm]). However, the variation in the estimated values was 0.08 when input impedance was measured repeatedly under the condition of L = 2.00 mm. Thus, we can also assume that this value is typically small. Moreover, the mean value obtained using the three different measurement methods was 7.2. Accordingly, each measurement value indicates that the difference in permittivity was within 0.4. The measurement results with isopropanol inserted can also be examined using the procedure described above.

Table 5. Complex permittivity of tap water with various L-dimension values (at 2.49806 GHz)

L [mm]	Newly evaluated coaxial line method [17]	TM_{010} cylindrical cavity resonator method [8]	Cut-off circular waveguide reflection method [14] – [16]
0.00	72.87 ± 1.03 – j6.98 ± 0.39	73.2 ± 0.4 – j7.5 ± 0.8	73.55 ± 0.93 – j8.49 ± 0.41
1.00	74.20 ± 0.62 – j9.01 ± 0.27		
2.00	72.16 ± 0.08 – j7.78 ± 0.47		

Table 6. Complex permittivity of methanol with various L-dimension values (at 2.5314 GHz)

L [mm]	Newly evaluated coaxial line method [17]	TM_{010} cylindrical cavity resonator method [8]	Cut-off circular waveguide reflection method [14] – [16]
0.00	23.30 ± 0.43 –j13.58± 0.55	22.1 ± 1.3 – j11.4 ± 2.1	21.33 ± 0.50 –j13.77±0.10
1.00	22.49 ± 0.26 –j13.14± 0.20		
2.00	22.07 ± 0.06 –j12.68± 0.17		

Table 7. Complex permittivity of ethanol with various L-dimension values (at 2.5395 GHz)

L [mm]	Newly evaluated coaxial line method [17]	TM_{010} cylindrical cavity resonator method [8]	Cut-off circular waveguide reflection method [14] – [16]
0.00	7.39 ± 0.05 – j7.92 ± 0.14	6.3 ± 0.3 – j6.8 ± 0.3	6.26 ± 0.18 –j7.13±0.18
1.00	7.48 ± 0.31 – j 7.46 ± 0.29		
2.00	7.40 ± 0.07 – j 7.20 ± 0.08		

Table 8. Complex permittivity of isopropanol (IPA) with various L-dimension values (at 2.5415 GHz)

L [mm]	Newly evaluated coaxial line method [17]	TM_{010} cylindrical cavity resonator method [8]	Cut-off circular waveguide reflection method [14] – [16]
0.00	3.06 ± 0.08 – j2.97 ± 0.12	3.5 ± 0.5 – j3.0 ± 0.1	3.24 ± 0.19 – j3.04 ± 0.05
1.00	3.44 ± 0.02 –j 2.76 ± 0.06		
2.00	3.58 ± 0.05 –j 2.74 ± 0.09		

Next, the complex permittivities of tap water, methanol, ethanol and isopropanol were also measured multiple times with the measurement jig filled with liquid to the coaxial line section under center conductor lengths of 0 to 2 mm with a low frequency band of 100 MHz. The results obtained using the proposed method with these lengths were compared to those of another measurement method. Tables 9 to 12 show the measurement results. Overall and individual consideration of the data obtained showed significant variations in the outcomes of complex permittivity estimation using the open-ended cut-off waveguide reflection method and the proposed method with L = 0.00 mm. However, variability was minimal when complex permittivity was measured using the proposed method with L = 1.00 and 2.00 mm. These results are attributable to the fact that the input impedance was almost open (∞Ω) [16] due to the patulous condition of the coaxial line's tip with L = 0 mm. Meanwhile, complex input impedance became finite due to electromagnetic wave absorption in this region because liquid was inserted to the coaxial line part with L = 1.00 and 2.00 mm. For each case shown in Tables 9 to 12, the measurement results indicate that the input impedance on the reference plane differed from the results obtained with the open-ended cut-off circular waveguide reflection method [16] more as the length of the center conductor increased. Meanwhile, the variation of the measurement values obtained with the newly evaluated method decreased as the length of the center conductor increased. Specifically, the variation in the estimated values of permittivity for tap water was 1.45 for the real part and 0.90 for the imaginary part with the length of the coaxial line's center conductor at L = 0.00mm (where the center conductor did not extend into the cylindrical cavity) when input impedance was measured repeatedly using the coaxial line reflection method in the low-frequency band of 100 MHz, as shown in **Table 9**. This variation was large. The variation in the measured values of permittivity was also large (1.21 for the real part and 1.87 for the imaginary part) when input impedance was measured repeatedly using the cut-off circular waveguide reflection method. However, this value was small (0.51 for the real part and 0.20 for the imaginary part) when the center conductor length was L = 1.00 mm with the coaxial line reflection method. Moreover, the variation in estimated values was 0.35 for the real part and 0.07 for the imaginary part under the condition of L = 2.00 mm. Based on these results, it was confirmed that variation decreased as the length of the center conductor increased. In addition, each measured value with the coaxial line's center conductor at lengths L = 1.00 and 2.00 mm corresponded to within 1.0 for the imaginary part. However, the difference was 3.0 with the length of the coaxial line's center conductor at L = 0.00 mm. These observations indicated that the value obtained when the center conductor was longer was more reliable. Next, the variation in the measured values of permittivity was 1.64 for the real part and 0.09 for the imaginary part with the coaxial line's center conductor in the cylindrical cavity with a length of L = 0.00 mm when input impedance was measured repeatedly with methanol, as shown in **Table 10**. Meanwhile, it was confirmed that the variation in measurement values was large (1.02 for the real part and 0.98 for the imaginary part). However, the variation in both real and imaginary values was small (0.68 for the real part and 0.63 for the imaginary part) when the center conductor length was L = 1.00 mm with the coaxial line reflection method. Moreover, the variations were 0.38 for the real part and 0.07 for the imaginary part when L = 2.00 mm. Thus, it was confirmed that the variation in the measurement values obtained with the coaxial line reflection method decreased as the length of the center conductor increased. Moreover, the difference in measurement values when L = 1.00, 2.00 and 0.00 mm was 2.0 for the real part and 1.0 for the imaginary part with the coaxial line reflection method. Thus it was confirmed that the value obtained when the center conductor was longer was more reliable.

Next, the variation in the estimated values of permittivity for ethanol was large (4.37 for the real part and 1.18 for the imaginary part) with the length of the coaxial line's center conductor in the cylindrical cavity at L = 0.00 mm when input impedance was measured repeatedly using the coaxial line reflection method, as shown in **Table 11**. It was additionally confirmed that the variation with the cut-off circular waveguide reflection method was also large (3.92 for the real part and 1.49 for the imaginary part). However, the variation was 1.02 for the real part and 0.87 for the imaginary part at L = 1.00 mm. Moreover, the variation was 0.60 for the real part and 0.23 for the imaginary part under the condition of L = 2.00 mm. The results confirmed that variation was reduced as the length of the center conductor increased. Moreover, the difference in measurement values obtained with center conductor lengths of L = 1.00, 2.00 and 0.00 mm was 1.1 for the real part using the coaxial line reflection method. Thus it was confirmed that the value obtained when the center conductor was longer was more reliable. The results obtained with isopropanol inserted can also be examined using the procedure described above.

Thus, the measurement values obtained with liquid inserted to the coaxial line part are more probable than those obtained using the cut-off circular waveguide reflection method involving a coaxial feed in a low-frequency band. It can therefore be inferred that the proposed method [17, 18] results in higher measurement precision with lower variability of complex permittivity for liquids than the open-ended cut-off circular waveguide reflection method [14] – [16].

Table 9. Complex permittivity of tap water with various L-dimension values (at 100 MHz)

L [mm]	Newly evaluated coaxial line method [17]	Cut-off circular waveguide reflection method [14] – [16]
0.00	79.92 ± 1.45 – j 2.07 ± 0.90	80.17 ± 1.21 – j 3.33 ± 1.87
1.00	79.30 ± 0.51 – j 4.64 ± 0.20	
2.00	80.11 ± 0.35 – j5.02 ± 0.07	

Table 10. Complex permittivity of methanol with various L-dimension values (at 100 MHz)

L [mm]	Newly evaluated coaxial line method [17]	Cut-off circular waveguide reflection method [14] – [16]
0.00	32.62 ± 1.64 – j 2.32 ± 0.09	33.48 ± 1.02 – j 1.84 ± 0.98
1.00	34.51 ± 0.68 – j 1.15 ± 0.63	
2.00	34.60 ± 0.38 – j 1.14 ± 0.07	

Table 11. Complex permittivity of ethanol with various L-dimension values (at 100 MHz)

L [mm]	Newly evaluated coaxial line method [17]	Cut-off circular waveguide reflection method [14] – [16]
0.00	26.29 ± 4.37 – j 3.00 ± 1.18	26.74 ± 3.92 – j 1.67 ± 1.49
1.00	25.12 ± 1.02 – j 2.90 ± 0.87	
2.00	24.66 ± 0.60 – j 2.60 ± 0.23	

Table 12. Complex permittivity of isopropanol (IPA) with various L-dimension values (at 100 MHz)

L [mm]	Newly evaluated coaxial line method [17]	Cut-off circular waveguide reflection method [14] – [16]
0.00	18.02 ± 3.67 – j 5.80 ± 5.00	18.30 ± 1.82 – j 6.24 ± 2.22
1.00	16.38 ± 0.20 – j 3.14 ± 0.13	
2.00	16.81 ± 0.40 – j 3.27 ± 0.13	

7. Frequency characteristics of complex permittivity in certain liquid types

The results of the study confirmed the proposed method's applicability to the measurement of complex permittivity for high-loss liquids over a wide range of frequencies from low to high. Accordingly, the complex permittivity of certain liquid types was subsequently measured using the proposed coaxial line method and cut-off waveguide reflection method under the conditions of 2b = 4.10 mm, 2a = 1.30 mm, L = 0 to 2.0 mm and ε_{rA} = 2.05 at frequencies ranging from 50 MHz to 3.0 GHz. In addition, the ambient temperature was 25.0°C for input impedance measurement with the both measurement methods.

The results of frequency characteristic measurement for complex permittivity using the newly evaluated method with different center conductor lengths are shown in Figs. 5 to 8 along with results obtained using the open-ended cut-off circular waveguide method. The estimated results data were overwritten repeatedly based on the results of frequency characteristic measurement for complex permittivity with center conductor lengths of L = 0.00, 1.00 and 2.00 mm. Figures 5 to 8 show estimated results for the frequency characteristics of complex permittivity for tap water, methanol, ethanol (99.5), and isopropanol, respectively. The outcomes indicate that frequency characteristics and other results for liquids as measured using the proposed method corresponded closely to those obtained using open-ended circular waveguide reflection method. Separate analysis of the measurement results for each liquid is outlined below. Figure 5 indicates that the real and imaginary parts of the complex permittivity of tap water were 80.0 to 71.0 and 2.0 to 9.0, respectively.

The corresponding figures for methanol were 34.0 to 19.0 and 1.0 to 14.0, those for ethanol (99.5) were 24.0 to 6.0 and 11.0 to 3.0, and those for IPA were 17.0 to 4.0 and 8.0 to 3.0. This indicates that the measurement results obtained using proposed method are in close agreement with those obtained using the previously proposed open-ended cut-off circular waveguide reflection method, including the determination of frequency characteristics. In particular, it was confirmed that the variation in complex permittivity values exceeded 2.0 for the real part with a center conductor length of L = 0.00 mm at a low frequency of around 100 MHz when tap water was inserted, as shown in Figure 5. Moreover, sometimes measurement could not be performed at a frequency of 100 MHz because input impedance was very high. However, the variations in measurement values were reduced to within 1.0 by extending the length of the center conductor. Next, Figure 6 shows that variation in the permittivity values of methanol exceeded 2.0 for the real part under the condition of L = 0.00 mm at around 100 MHz. However, the variation in measurement values was also reduced to within 1.0 by extending the length of the center conductor. The results shown in Figures 7 and 8 also show that the variation in measurement values was large under the condition of L = 0.00 mm at low frequencies. However, the variation in measurement values was also reduced to within 1.0 by extending the length of the center conductor.

The frequency range measurable with the coaxial line reflection method depended on the following conditions regarding the structure of the jig. The minimum frequency was subject to the length of the center conductor. However, the maximum frequency was subject to the length of the center conductor and the cut-off frequency of the first higher mode propagation, which was determined by the outside dimensions of the sample insertion space. The reason for this is that resonance phenomena appear when the coaxial length is 1/4λ. Therefore, measurement should be performed at a frequency lower than this resonance condition. In this study, an SMA connector was chosen for the construction of the measurement jig. Accordingly, the length of the center conductor in the cylindrical cavity dipped in liquid was set at L = 0 to 2 mm to avoid

resonance phenomena at high frequencies. Therefore, the measurement frequency range for measurement of the input impedance with the coaxial line reflection method was set at 50 MHz to 3 GHz. Meanwhile, measurement at lower frequencies was achieved by extending the length of the center conductor. However, measurement of input impedance depended not only on the dimensions of the jig but also on the calculation procedures, especially at high frequencies. Therefore, there is a need for research in the near future on frequency ranges measurable with this method at frequencies other than those used in this study.

It can be concluded that the newly evaluated method [17, 18] offers higher precision in the measurement of complex permittivity for liquids than the open-ended cut-off circular waveguide reflection method [14] – [16] because the variation of the measurement values obtained with the newly evaluated method decreased as the length of the center conductor in the low-frequency band. It was additionally confirmed that the structure of the jig with the coaxial line part filled with liquid leads to improved accuracy in the measurement of complex permittivity for high-permittivity high-loss liquids at low frequency.

Measurement uncertainty would be an applicable metric for evaluating the measurement accuracy of the proposed method. However, variation in this study was instead evaluated quantitatively using values obtained from repeated measurement of input impedance under each condition. This was because the major purpose of the study was to clarify the validity of the proposed method for certain types of liquids in a broad frequency range based on comparison of measurement results with those of another method. The variation in measurement values regarding measurement uncertainty was caused by the accumulation of many factors, such as the calibration of S_{11}, the dimensions of the jig, the accuracy of numerical calculation, the condition of the connection, variation in the state of the cable, and the repeatability of the sample insertion conditions. Therefore, further study of these factors is needed to specify measurement uncertainty with this method.

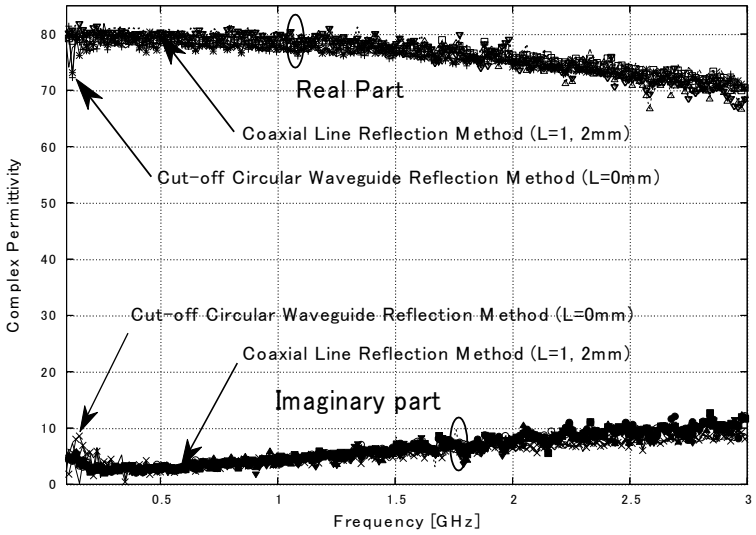

Figure 5. Frequency characteristics of complex permittivity (tap water)

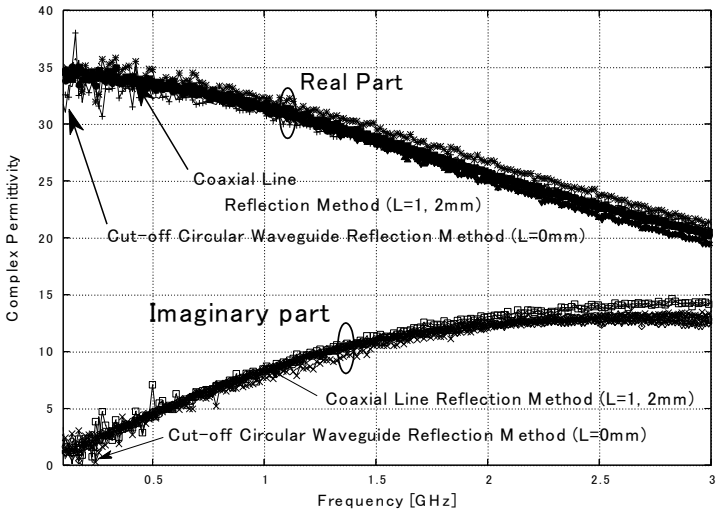

Figure 6. Frequency characteristics of complex permittivity (methanol)

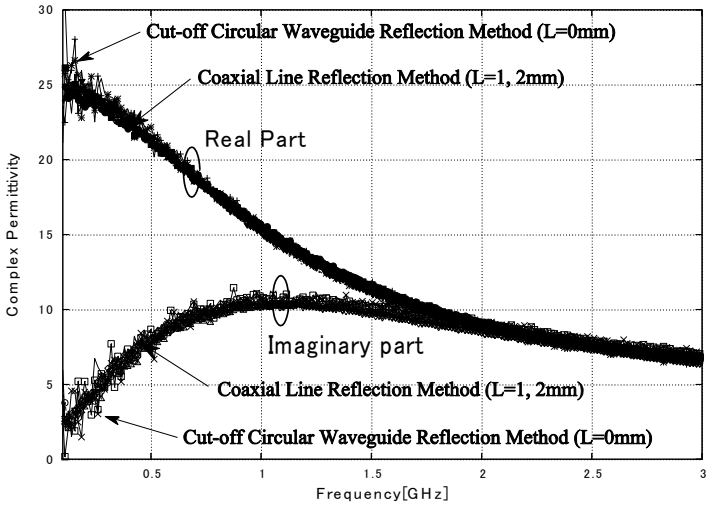

Figure 7. Frequency characteristics of complex permittivity (ethanol 99.5)

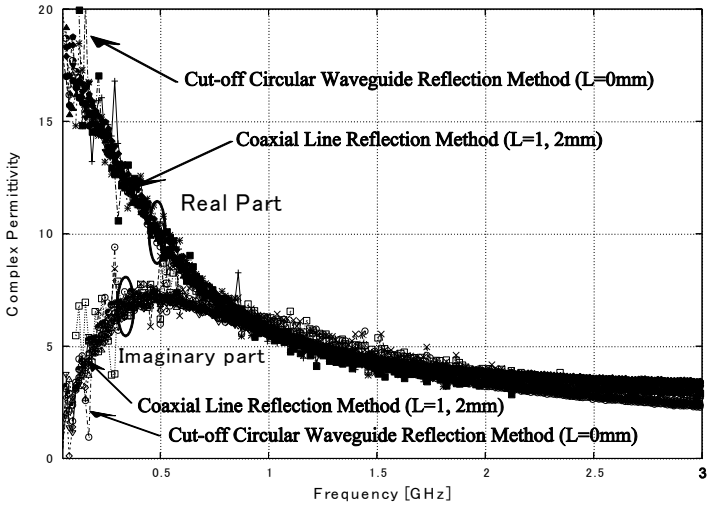

Figure 8. Frequency characteristics of complex permittivity (IPA)

8. Conclusion

This study involved the verification of a method for broadband measurement to determine the complex permittivity of liquids using the reflection method with an open-ended circular cut-off waveguide and a coaxial line as an SMA connector feed. The complex permittivities of tap water, methanol, ethanol and IPA were estimated from measured input impedance values using a vector network analyzer. The measurement results were compared with outcomes obtained using the cylindrical cavity resonator method and the open-ended circular cut-off waveguide method (as previously proposed by the authors) to evaluate the effectiveness of the proposed technique and the open-ended circular cut-off waveguide method, respectively. The extent to which center conductor filling with liquid to different lengths influenced measurement results was also evaluated. Based on the outcomes, the frequency characteristics of the complex permittivity of certain types of high-loss liquids were determined at frequencies ranging from 50 MHz to 3.0 GHz on the basis of the measurement procedure outlined above. It was confirmed that complex permittivity in high-permittivity and high-loss liquids can be measured at lower frequencies using a jig with a liquid-filled coaxial line part than a state in which the center conductor of the coaxial line is not filled with liquid. It was also concluded that this structure leads to improved measurement accuracy at low frequencies.

In future work, further jig improvement with a large-diameter coaxial line and a material insertion space at low frequency is needed. The temperature dependence of these liquids will also be studied using the proposed method. In particular, in future work, more precise measurement of the temperature characteristics of complex permittivity in various liquids should be performed with strict temperature controls to develop better measurement environments. Highly accurate numerical analysis for the open-ended section is also needed to deal with low-loss materials. Research to extend the method to the measurement of liquids in the millimeter band is also required.

References

1) K. Fukunaga, S. Watanabe, K. Wake and Y. Yamanaka, “Time dependence of tissue-equivalent dielectric liquid materials and its effect on SAR,” Proc. of Int. Symposium on Electromagnetic Compatibility, Sorrento, Italia, pp. 763-767, 2002-9.
2) A. Hirata, S. Kodera, J. Wang, and O. Fujiwara, “Dominant factors for influencing whole-body average SAR due to far-field exposure in whole-body resonance frequency and GHz regions, ” Bioelectromagnetics, vol.28, pp.484-487, 2007.
3) H. Shimizu, Y. Yoshimura, H. Hinou, and S. Nishimura, “A new glycosylation method part 3: study of microwave effects at low temperatures to control reaction pathways and reduce by products,” Tetrahedron Vol.64, Issue 43, 10091-10096, 2008-10.
4) K. Huang, X. Cao, C. Liu and X.-B. Xu, “Measurement / Computation of Effective Permittivity of Dilute Solution in Saponification Reaction, ” IEEE Trans. Microw. Theory Tech. Vol. MTT-51, No. 10, pp.2106-2111, 2003-10.
5) J. R. Mosig and J. C. Ebesson, “Reflection of an open- ended coaxial line and application to nondestructive measurement of materials,” IEEE Trans. on Instru. and Meas., Vol. IM-30, No. 1, pp. 46 – 51, 1981-3.
6) C. P. Chen, Y. Dong, M. Niu, D. Xu, Z. Ma and T. Anada, “In-Situ Measurement of Complex EM Parameters of Dispersive Absorbing Materials by Coaxial-Probe-Based Frequency-Variation Method,” IEICE Trans. Electron., Vol. E89-C, No. 12, pp. 1814 – 1820, 2006-12.
7) S. Li and R. G. Bosisio, “Composite hole conditions on complex permittivity measurements using microwave cavity perturbation,” IEEE Trans. Microw. Theory Tech., Vol. 30, No. 1, pp. 100 – 104, 1982-1.
8) A. B. Maslenikov and A. S. Omar, “Accurate microwave resonant method for complex permittivity measurements of liquids,” IEEE Trans. Microw. Theory Tech., Vol. 48, No. 11, pp. 2159 – 2164, 2000-11.
9) Y. Kuriyama, N. Ueda, A. Nishikata, K. Fukunaga, S. Watanabe and Y. Yamanaka, “Liquid Material’s Complex Permittivity Measurement Using a Rectangular Waveguide and a Dielectric Tube at 800 and 900MHz band,” Proc. of Int. Symp. on Electromagnetic Compatibility, Sendai, Japan, vol. 2, pp.645-648, 2004-6.

10) K. Shibata, K. Tani, O. Hashimoto and K. Wada, “Measurement of Complex Permittivity for Liquid Phantom by Transmission Line Method Using Coaxial Line,” IEICE Trans. Electron., Vol. E87-C, No. 5, pp. 689 – 693, 2004-5.
11) E. Kushizaki, J. Chakarothai, Q. Chen, K. Sawaya and M. Suzuki, “A Study on Liquid Permittivity Measurement Using a Cylindrical Cavity,” IEICE Tokyo Japan, Tech. Rep., Vol. 108, No. 132, EMCJ 2008-37, pp. 67 – 70, 2008-7 (in Japanese).
12) T. Michiyama, E. Tanabe and Y. Nikawa, “Complex Permittivity Measurement for Lossy Materials Using an Obliquely Cut Open-ended Coaxial Probe,” IEICE Trans. Electron., Vol. J89-C, No. 12, pp. 1082 – 1084, 2006-12 (in Japanese).
13) N. E. Belhadj-Tahar and A. F. Lamer, “Broad-Band Analysis of a Coaxial Discontinuity Used for Dielectric Measurements,” IEEE Trans. Microw. Theory Tech., Vol. MTT-34, No. 3, pp. 346 – 349, 1986-3.
14) K. Shibata, “Measurement of Complex Permittivity for Liquid Materials Using the Open-ended Cut-off Waveguide Reflection Method,” IEICE Trans. Electron., Vol. E93-C, No. 11, pp. 1621 – 1629, 2010-11.
15) K. Shibata, “Measurement of Complex Permittivity for Liquid Materials Using the Open-ended Cut-off Waveguide Reflection Method,” Proc. of 2011 China-Japan Joint Microwave Conference, CJMW2011, Hangzhou, China, pp.1-4, 2011-4.
16) K. Shibata, “Broadband Measurement of Complex Permittivity for Liquids Using the Open-ended Cut- off Circular Waveguide Reflection Method,” 35th PIERS Proceedings, Guangzhou, China, pp. 2089 – 2084, 2014-8.
17) J. B. Jarvis, M. D. Janezic and C. A. Jones, “Shielded Open-circuited Sample Holder for Dielectric Measurements of Solids and Liquids,” IEEE Trans. Instru. and Meas., Vol. IM-47, No. 2, pp. 338 – 344, 1998-4.
18) K. Shibata and J. Kamiyama, “Fundamental Study on Measurement of Complex Permittivity for Liquid Materials Using the Open-ended Coaxial Waveguide Reflection Method,” (in Japanese), IEICE Tokyo Japan, Tech. Rep., Vol. EMCJ 2009-57, MW 2009-106, pp. 75 – 80, 2009-10.
19) W. H. Press, S. A. Teukolsky, W. T. Vetterling and B. P. Flannery, “Numerical Recipes in Fortran 77 Second edition,” Cambridge University Press, pp. 372 – 375, 1992.
20) T. J. Ypma, “Historical development of the Newton-Raphson method,” *SIAM Review* **37** (4), 531 –551, 1995.
21) A. P. Gregory, Y. Johnson, K. Fukunaga, R. N. Clarke and A. W. Preece, "Traceable Dielectric Measurements of New Liquids for Specific Absorption Rate (SAR) Measurement in the Frequency Range 300 MHz to 6 GHz," Proc. Conference on Precision Electromagnetic Measurements, W2d4, U.K., pp.425-428, 2004-7.

要　旨

近年電磁波による人体影響が懸念されており、この影響を調べる基礎検討として液体ファントムの複素誘電率を測定する研究等が行われている。本研究では充填時の液漏れの影響を軽減することを目的として同軸給電による終端を開放した遮断円筒導波管を装荷した同軸線路を用いた反射波法により、まず水道水、エタノール、メタノールおよびイソプロピルアルコールの複素誘電率の測定を行い、円筒空洞共振器および終端開放遮断円筒導波管反射法による結果と比較して両者が良好に一致することを確認した。その際、反射係数の数値計算はモード整合法を適用した。更に、同軸線路長の違いによる複素誘電率への影響ついても検討を行った。そして、これらの基礎検討をもとに 0.5～3.0GHz の周波数帯においてエタノール、メタノールおよび IPA の複素誘電率を測定した。その結果、各種の高損失な液体材料の複素誘電率の周波数特性を把握することが出来た。

キーワード: 誘電率測定, 液体, 同軸線路, 遮断導波管, 円筒空洞共振器, モード整合理論, モード整合法, モード解析, 固有モード展開, 電磁界解析, 測定標準